30 Mar 2001, 1:30 pm - 3:30 pm

Effective Stress Analysis by Shear Strain Controllable Model and its Application to Centrifuge Shaking Model Test

Hiroki Kurose
Tokyo Electric Power Services Co., Ltd., Japan

Masayuki Sato
Tokyo Electric Power Services Co., Ltd., Japan

Hitoshi Azuma
Tokyo Electric Power Services Co., Ltd., Japan

Katsumi Ozeki
Tokyo Electric Power Services Co., Ltd., Japan

Nozomu Yoshida
Sato Kogyo Co., Ltd., Japan

Effective Stress Analysis by Shear Strain Controllable Model and its Application to Centrifuge Shaking Model Test

Hiroki Kurose, Masayuki Sato, Hitoshi Azuma, Katsumi Ozeki
Tokyo Electric Power Services Co., Ltd. Japan

Nozomu Yoshida
Sato Kogyo Co., Ltd. Japan

ABSTRACT

Effective stress FEM which is able to control the growth of shear strains is proposed. Its validity is firstly confirmed through the simulation of undrained cyclic torsional shear tests. Then, it is applied to simulation of centrifuge shaking model tests; the experimental model consists of a caisson type quay wall and reclamation laid on the sand layer. Development of shear strain is shown to be controlled arbitrary keeping the excess porewater pressure generation unchanged through the simulation of undrained cyclic torsional shear test, which indicates that proposed model can be applicable to variety of soils with different density and fines contents. Displacement is shown to be controlled keeping excess porewater pressure generation constant in the centrifugal model, too, and good agreement is obtained between test and analysis by controlling the parameter for shear strain development.

INTRODUCTION

Effective stress FEM has been widely used to predict onset of the liquefaction in the saturated cohesionless soil during earthquake. Consequently, prediction of excess porewater pressures was primary interest. Recently, however, effective stress FEM comes to be used to evaluate deformations of the ground and the structures during and after liquefaction, so that not only excess porewater pressure but also growth of strains in soil layer are required to predict in the effective stress FEM. From this point of view, constitutive low that is able to control both excess porewater pressure generation and shear strain growth after liquefaction is developed for various types of liquefiable soil behaviors such as loose sand, dense sand, silty sand etc.

SHEAR STRAIN CONTROLLABLE MODEL

The constitutive model developed by Tobita and Yoshida (1994) are modified to achieve strain controllable feature. The computer code STADAS (Yoshida, 1993) that installs target constitutive model is modified to improve constitutive model and renamed STADAS II.

Basic Equations

The yield surface is expressed as follows:

$$f_M(\sigma_{ij}, \mu_M) = 0 \tag{1}$$

where μ is a scalar hardening parameter. The subscript M is used in order to signify the normal (maximum) yield surface. The stress-dilatancy equation based on the energy dissipation is expressed as follows (Gutierrez, 1989):

$$s_{ij} e^p_{ij} - p\varepsilon^p_v + = pM\xi \tag{2}$$

where s_{ij} denotes the deviatric stress, e_{ij} denotes the deviatric strain, ε_v denotes the volumetric strain, and M is a material parameter.

The hardening modulus H_P in cyclic plasticity region is expressed as follows:

$$H_P = H_R - \left(H_R - H^*_P\right) \cdot \left(\frac{\rho}{\rho_c}\right)^m \tag{3}$$

where m is a material constant; H^*_P is the plastic modulus on the bounding surface, that is kept constant as far as cyclic plasticity within the bounding surface continues. H_R is a hardening modulus reflecting the effect of accumulated shear strain within a course of cyclic plasticity.

Modification from Basic Equation

In the effective stress FEM, shear modulus is usually given by a power function of effective mean stress as follows:

$$G = G_0 \left(\frac{\sigma'_m}{\sigma'_{m0}}\right)^n \tag{4}$$

where G_0 is an initial shear modulus at $\sigma'_m = \sigma'_{m0}$, σ'_m is an effective confining stress, σ'_{m0} is an initial effective confining stress and n is a parameter usually used as n=0.5.

Figure 1 shows a result of an undrained cyclic torsional shear test on Toyoura sand with relative density Dr=65% carried out

by the authors. Figures 1(a) and (b) show the effective stress pass and shear stress strain curve respectively. Figure 2 shows a relationship between G/G_0 and effective stress ratio σ'_m / σ'_{m0}, in which G is a modulus at shear strain is zero. In the earlier stage of the test, from the initial step to the step where σ'_m / σ'_{m0} falls down to half of σ'_{m0}, computed G/G_0 agrees with test result, which indicates n=0.5. However, when σ'_m / σ'_{m0} is smaller than 0.5, the test result gradually becomes smaller than the line of n=0.5. In order to express this phenomena, G is modified from Eq. (4).

$$G = G_0 \left(\frac{\sigma'_m}{\sigma'_{m0}} \right)^n \cdot \left(1 - \frac{\alpha}{B} \right)^c \tag{5}$$

Here α is defined as

$$\alpha = \sigma_e / \sigma'_m, \quad \sigma_e = \sqrt{3/2 s_{ij} s_{ij}} \tag{6}$$

and B is defined as

$$B = \sqrt{3} \sin \phi_f \tag{7}$$

where ϕ_f is a shear resistance angle and c is a parameter.

By using Eq. (5), shear modulus G degrades extremely when the stress pass closely approaches to the failure lines, leading to rapid increase of shear strain. Consequently, the rate of increase of shear strain due to a rise of excess porewater pressure can be controlled by altering parameter c in Eq. (5).

Equation (3) can be rewritten in the form.

$$H_P = H_R \cdot \left[1 - \left(\frac{\rho}{\rho_c} \right)^m \right] + H_p^* \left(\frac{\rho}{\rho_c} \right)^m \tag{3}'$$

This is modified to be

$$H_P = H_R \cdot \left[1 - \left(\frac{\rho}{\rho_c} \right)^m \right] \cdot \Delta^\beta \cdot \left(\frac{N}{N_1} \right)^s + H_p^* \left(\frac{\rho}{\rho_c} \right)^m \tag{8}$$

where N_1 is a number of cycles causing liquefaction at reference stress ratio obtained from laboratory test. N is a number of cycles causing liquefaction at present stress ratio. Parameters Δ and s are expressed as follows:

$$\Delta = \begin{cases} 1.0 & 0 \le \dfrac{\alpha}{M} \le 1.0 \\ \dfrac{B-\alpha}{B-M} & 1.0 < \dfrac{\alpha}{M} < \dfrac{B}{M} \end{cases} \tag{9}$$

$$s = \begin{cases} 1.0 + (s_1 - 1.0) \cdot \dfrac{\alpha}{M} & 0 \le \dfrac{\alpha}{M} \le 1.0 \\ \dfrac{s_1}{d - 1.0} \cdot \left(d - \dfrac{\alpha}{M} \right) & 1.0 < \dfrac{\alpha}{M} < d \\ 0.0 & d < \dfrac{\alpha}{M} < \dfrac{B}{M} \end{cases} \tag{10}$$

where β, s_1 and d are material constant being to control the effective stress passes such as Fig. 1(a).

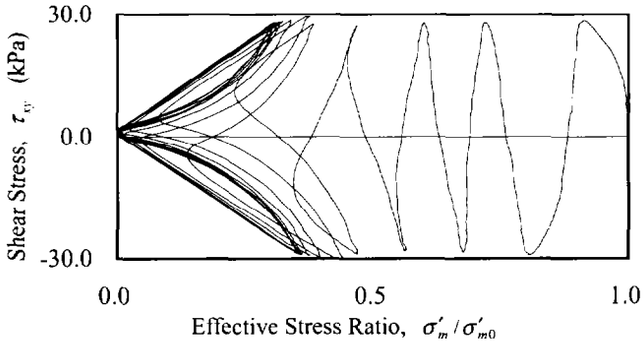

(a) Effective stress pass

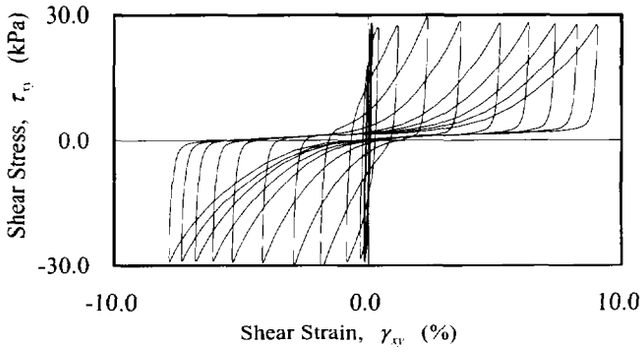

(b) Shear stress strain curve

Fig. 1 Results of undraind cyclic torsional shear test

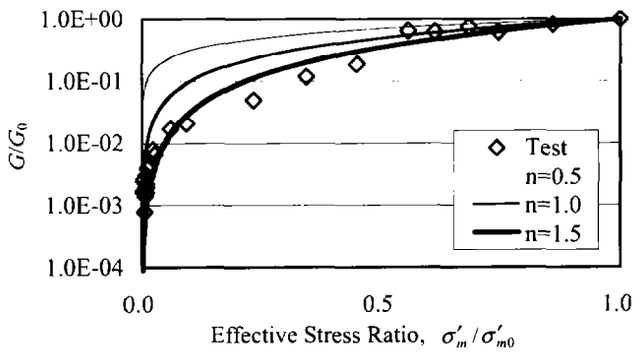

Fig. 2 Relationship shear modulus and effective stress ratio

CASE STURY ON UNDRAINED CYCLIC TORSIONAL SHEAR TEST

In order to examine the capability of the model, a case study is conducted to simulate undrained cyclic torsional shear test, in which the parameter c Eq. (5) is either 0.25 and 0.45. Other material parameters used in the simulations are listed in Table 1.

Figures 3 and 4 show effective stress passes and time histories of the excess porewater pressure in these cases. Analytical results are nearly identical in two cases, which indicates that the parameter c has almost no influence on the development of the excess porewater pressure. Moreover, by comparing with Fig. 1, it is recognized that this model represents cyclic mobility behavior in dense sand well.

Table 1 Material parameters

Parameters	Value
G_0	15000(kN/m^2)
K_0	29000(kN/m^2)
$B=\sqrt{3}\sin\phi$	1.403
β	1.6
m	0.023
s_1	1.0
d	2.8

$\sigma'_{m0}=\sigma_x=\sigma_y=98$kPa

x and y denote horizontal and vertical directions

G_0 and K_0 are given for $\sigma'_{m0}=98$kPa.

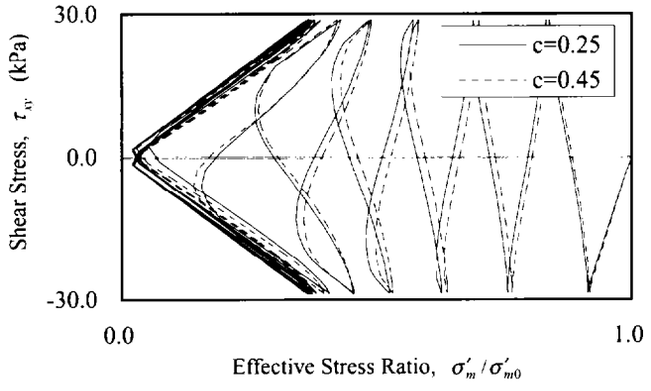

Fig. 3 Calculation results of stress pass

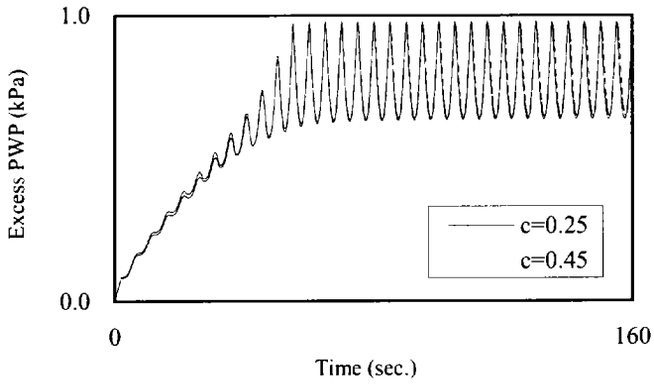

Fig. 4 Calculation results of excess porewater pressure

Figure 5 shows a comparison of shear strain time histories. Regardless of good agreement in excess porewater pressure, shear strain developments are quite different in two cases. Shear strain increases gradually when c=0.25, whereas it increases rapidly when c=0.45.

Figure 6 shows the analytical results of the relationship between cyclic shear stress ratio and number of cycles causing initial liquefaction (at which the excess porewater pressure reaches 95% of initial confining pressure) and those obtained from test. Number of cycles at which shear strain reaches 3% and 5% are also plotted. When c=0.25, number of cycles causing initial liquefaction is almost the same with that of 3% of shear strain, but number of cycles causing 5% of shear strains are approximately twice as that causing the initial

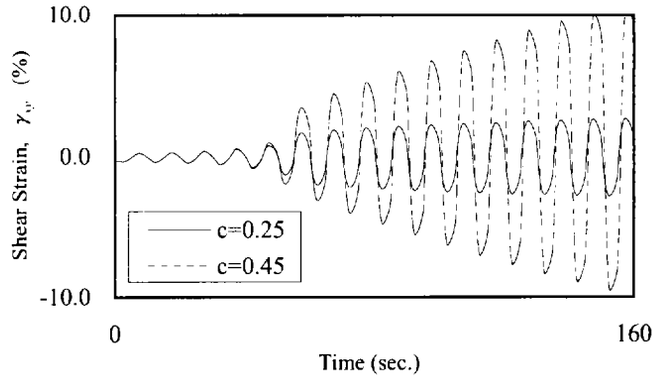

Fig. 5 Calculation results of shear strain

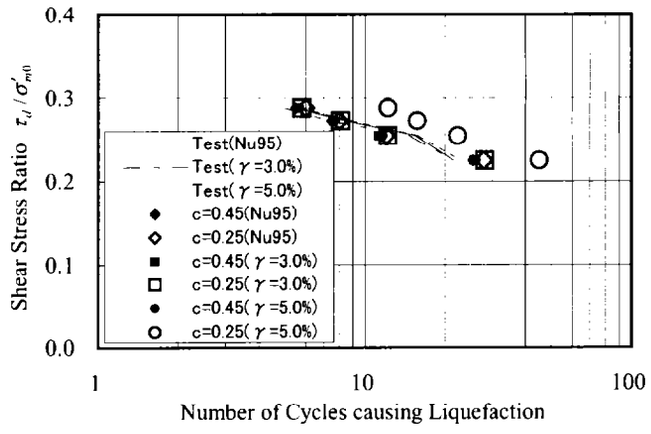

Fig. 6 Calculation results of the relationship between shear stress ratio and number of cycles causing liquefaction

liquefaction. On the other hand, when c=0.45, number of cycles of above mentioned 3 conditions have only a slight difference to each other, which phenomena agrees with test result such as Fig. 1.

From these results, it is clarified that parameter c can control the development of shear strain without changing excess porewater pressure generation, which means that this model may be applied to various kind (in density, fine contents etc.) of sandy soils. Stress strain curves of Toyoura sand with relative density between 30% and 80% are compared with the test results in Figs. 7 and 8. It is noted that the analysis expresses individual characteristics of different relative densities with fair accuracy.

NUMERICAL SIMULATIONS OF CENTRIFUGE SHAKNG MODEL TEST

Centrifuge Shaking Model Test

A rigid vessel made of aluminum plates with inner dimension of 110 cm long, 40 cm wide, and 30 cm high is fixed on the shaking table which is connected to a steel basket supported by a hinge at the end of rotating arm of about 6.5m in length.

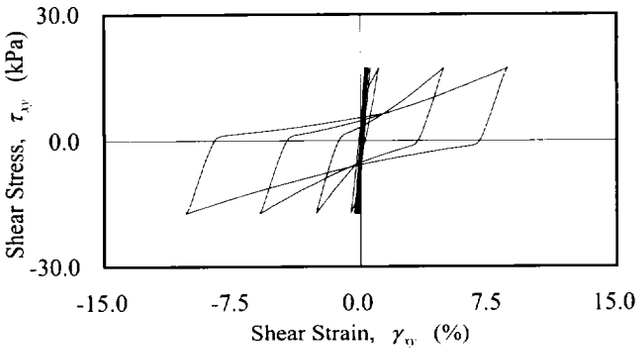

Fig.7(a) Calculation result of shear stress strain curve (Toyoura sand, Dr=30%)

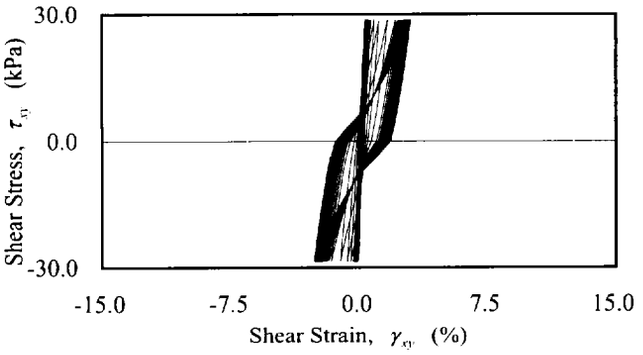

Fig.8(a) Calculation result of shear stress strain curve (Toyoura sand, Dr=80%)

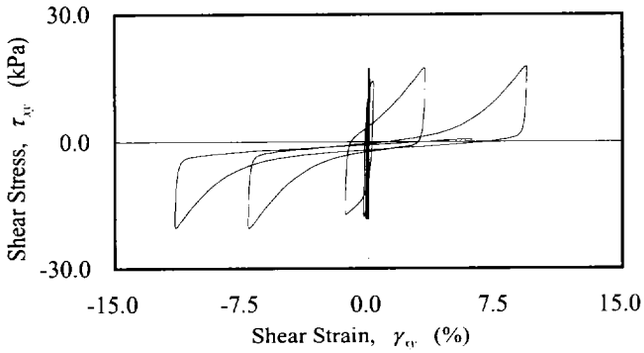

Fig.7(b) Testl result of shear stress strain curve (Toyoura sand, Dr=30%)

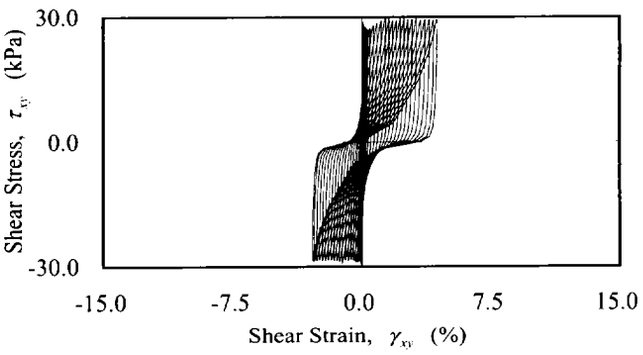

Fig.8(b) Test result of shear stress strain curve (Toyoura sand, Dr=80%)

Inside the vessel, the model consisting of a caisson, water saturated base layer, backfill soil and front water is installed as shown in Fig. 9. Structural element such as rubble mound and rubble backfilling are frequently installed in the actual structure, but they are not installed here in order to make the behavior simple. The water level is set at ground surface. Base layer and backfill soil is made of Toyoura sand whose relative density is 65%. The sand is poured into the rigid box, in which the caisson model had been set, by dry pluviation. Then silicon-oil is introduced to the soil through the inlet tube at the base of the rigid vessel which is put in the evacuated container. In the test, from the law of similarity, silicon-oil at 50 cSt dynamic coefficient of viscosity is used as the pore fluid. Sensors and measurement positions of the model are shown in Fig. 9. The models are subjected to sinusoidal acceleration with 150Hz and peak acceleration of 20g for 0.2 seconds. Gravity of acceleration in the centrifuge test is 50g.

Simulations

Table 2 shows cases of the numerical analysis. FEM mesh is shown in Fig. 10. Boundary conditions along the bottom and both sides are set to be fixed ones. As seen in Table 2, difference between four cases is parameter c. The most relevant value of c is evaluated 0.45 for 65% of Toyoura sand in the

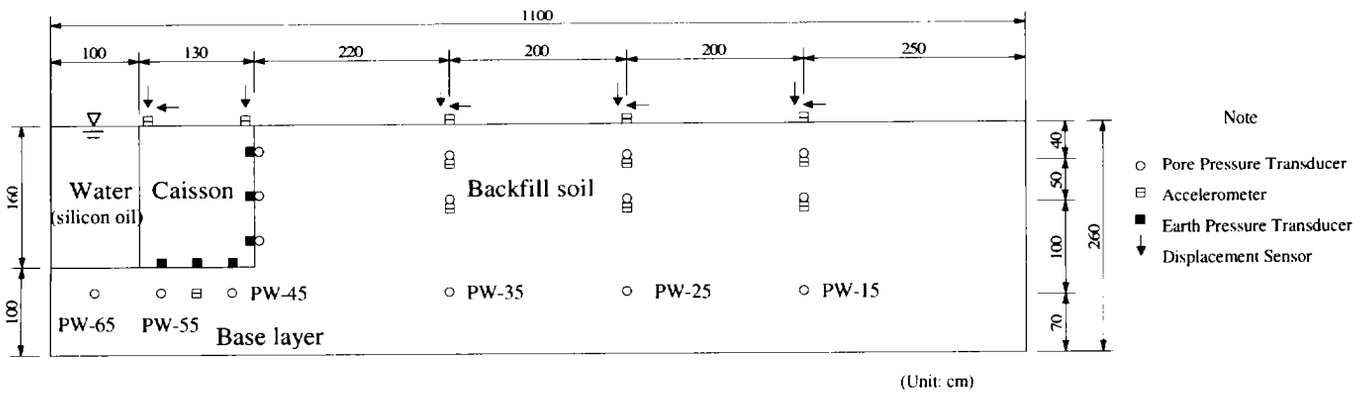

Fig.9 Model of centrifuge shaking model test

Table 2 Cases of numerical simulations

Case	value of parameter c
Case-1	0.15
Case-2	0.25
Case-3	0.35
Case-4	0.45

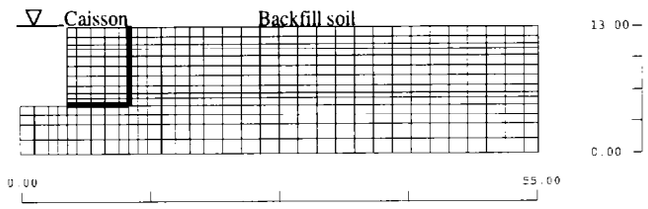

Fig.10 FEM mesh of this centrifuge shaking model test

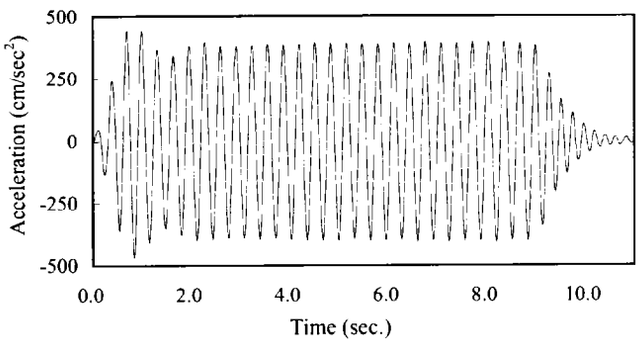

Fig.11 Base acceleration of test result and input acceleration of numerical simulations

preliminary study. Figure 11 shows a base acceleration measured in the test, which is used as the input motion in the numerical analysis. Peak acceleration of this time history is 441cm/sec^2.

Calculated time histories of horizontal acceleration at the top of the caisson in Case-2 (c=0.25) and Case-4 (c=0.45) are compared with the test result in Fig. 12. Both cases show similar behavior and agree with test result except the duration from 0.5 to 1.5 sec, in which analysis shows larger acceleration than observed regardless of the value of c.

Figure 13 shows the calculated time histories of the displacement at the bottom of the caisson. Both calculated results are in good agreement with the test results before 4 sec. However, after about 4sec, Case-2 and Case-4 have a remarkable difference from each other. While caisson's displacement stop at about 30cm in Case-2, it becomes larger gradually during whole excitation in Case-4. From this viewpoint, it may be said that the results of Case-4 agrees with the test results rather than that of Case-2. Residual displacement of the caisson in Case-2 is much smaller than the test result, whereas it is larger than test result in Case-4. There remains a question why the residual displacement of the caisson in Case-4 becomes larger than the test result, in spite good agreement in element test. The most possible reason may be the densification of soil in the centrifugal test at the time of install and gravity application, but it is not confirmed.

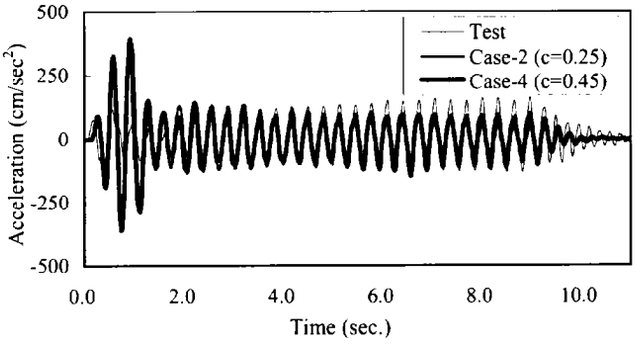

Fig.12 Horizontal acceleration time history of caisson

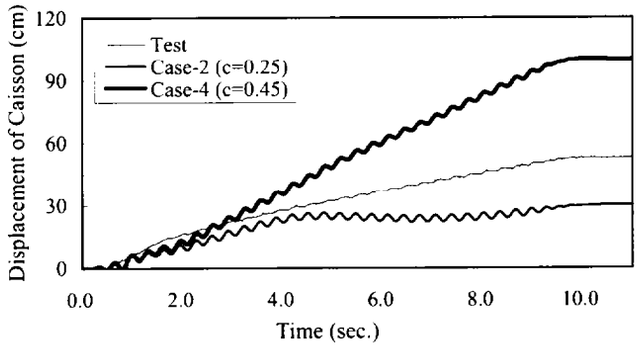

Fig.13 Horizontal displacement time history of caisson.

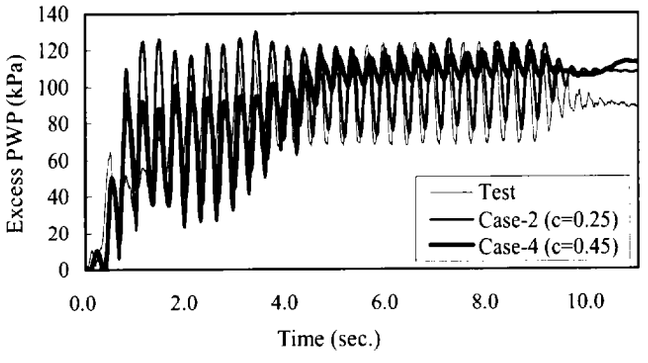

Fig.14(a) Excess porewater pressure time history (PW-25)

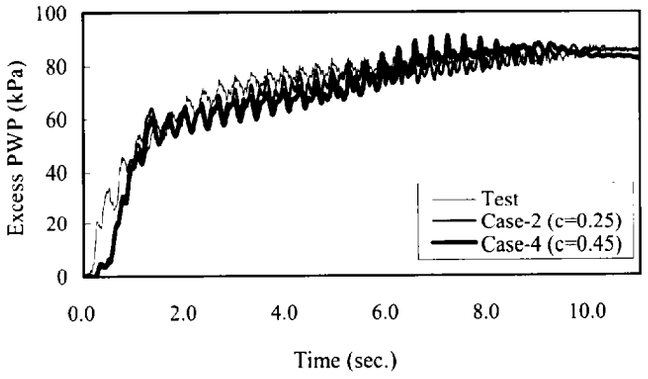

Fig.14(b) Excess porewater pressure time history (PW-45)

Figure 14 shows a comparison of time histories of the excess porewater pressures at the locations of PW-25 and PW-45 indicated in Fig. 9. At PW-25 that is located far from the

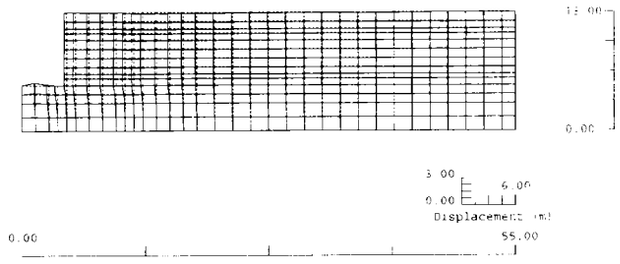

(a) Residual deformation

(b) Distribution of maximum excess porewater pressure ratio

Fig.15 Calculation results of Case-2 (c=0.25)

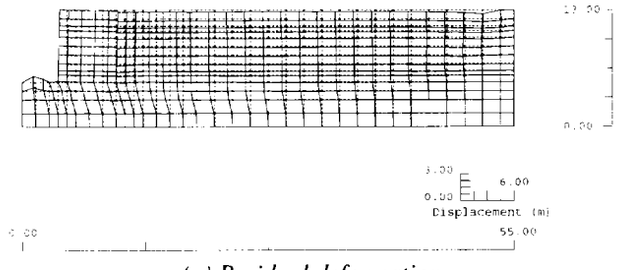

(a) Residual deformation

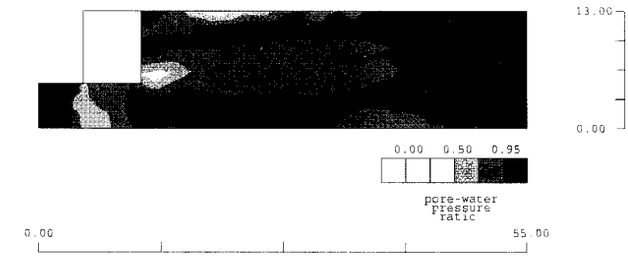

(b) Distribution of maximum excess porewater pressure ratio

Fig.16 Calculation results of Case-4 (c=0.45)

caisson, both analyses agree with the test result very well. However, at PW-45 that is located just below the caisson, Case-4 does not show the remarkable variation, in spite of the violent variation of the test result. It seems to indicate a characteristic feature of dense sand, particularly after 4sec when the displacement of the caisson in the analysis becomes less than that of test. In this point of view, the result of Case-2, which corresponds to denser sand, is more similar to the test result rather than that of Case-4.

Figures 15 and 16 show residual deformations and distributions of maximum excess porewater pressure ratio obtained from the numerical simulations. Excess porewater pressure near the caisson in Case-4 is smaller than that of Case-2 because of large movement of the caisson toward sea.

Figure 17 shows a relationship between the displacement of the caisson and parameter c. It is noted that the value of c has a considerable influence on the displacement of caisson and soil deformation.

CONCLUSION

Effective stress FEM is developed not only to predict the onset of the liquefaction but also to evaluate the deformation of the soil-structure systems during and after the liquefaction. Then the validity of the program is examined by the simulations on undrained cyclic torsional shear tests and centrifuge shaking model tests.

As a result, it is considered that the proposed method is applicable for various types of soils such as loose sand, dense sand and so on, by altering the specific parameter adopted in this study, which is able to control the growth of shear strain.

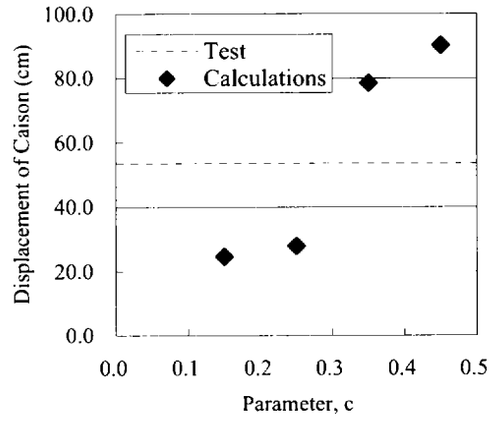

Fig.17 Relationship between displacement of caisson and parameter, c

REFERENCES

Tobita, Y. Yoshida, N. [1994]. An isotropic bounding surface model for undrained cyclic behavior of sand; Limitation and Modification, Proc. International Symposium on Pre-Failure Deformation of Geomaterials, Sapporo, pp.457-462.

Yoshida, N. [1993]. STADAS, A computer program for static and dynamic analysis of ground and soil-structure interaction problems, Report, Soil Dynamics Group, The University of British Columbia, Vancouver, Canada.

Gutierrez, M. [1989]. Behavior of Sand during rotation of Principal Stress Direction, D. Eng. Thesis, University of Tokyo.